Theor Chim Acta (1991) 78: 247–266

Theoretica Chimica Acta

Energy-adjusted *ab initio* pseudopotentials for the second and third row transition elements: molecular test for M_2 (M = Ag, Au) and MH (M = Ru, Os)

D. Andrae, U. Häußermann, M. Dolg, H. Stoll, and H. Preuß

Institute für Theoretische Chemie, Universität Stuttgart, Pfaffenwaldring 55, W-7000 Stuttgart 80, Federal Republic of Germany

Received May 28, 1990; received in revised form and accepted August 23, 1990

Summary. Recently published nonrelativistic and quasirelativistic energy-adjusted *ab initio* pseudopotentials representing the $M^{(Z-28)+}$ cores of the second row transition metal atoms and the $M^{(Z-60)+}$ cores of the third row transition metal atoms have been tested in SCF, CI(SD) and CEPA1 calculations of the spectroscopic constants (R_e, D_e, and ω_e) of the ground states of the neutral and singly charged silver and gold dimers, and in state averaged CASSCF and multireference CI(SD) calculations of the spectroscopic constants (R_e, D_e, ω_e, μ_e, $\partial\mu/\partial R$). Comparison is made with experimental and reliable theoretical data where available; in the case of the hydrides, additional calculations with pseudopotentials published by other groups have been made for comparison.

Key words: Pseudopotentials – Transition metals

1. Introduction

Transition metal (TM) compounds are of increasing importance in the whole field of chemistry, especially in organometallic chemistry, homogeneous and heterogeneous catalysis, and bioinorganic chemistry. Theoretical studies therefore are necessary for both predicting and interpreting experimental results. While the theoretical treatment of transition metal compounds at the all-electron level is very laborious, it is greatly facilitated when atomic pseudopotentials (PP) are used to represent the atomic core regions in molecular calculations, and only the "valence electrons" are treated explicitly [1–3]. Moreover, pseudopotentials provide a convenient and reliable tool for incorporating relativistic effects in molecular calculations. In a previous paper [4] we presented nonrelativistic Hartree–Fock (HF) and quasirelativistic Wood–Boring (WB) *ab initio* pseudopotentials that have been adjusted to the valence energies of a multitude of atomic many-electron reference states (HF-MEFIT-PP, WB-MEFIT-PP), together with the corresponding optimized valence GTO basis sets. In this way, second and third row TM atoms may be treated as 11- to 20-electron systems. Excitation and ionization energies from HF and SCF pseudopotential calculations using these basis sets differ by less than 0.1 eV from corresponding all-electron results for low-lying states of the atoms and singly charged positive

ions. However, since good atomic results do not always guarantee success in molecular calculations, the reliability of the pseudopotentials and the basis sets should be tested in calculations on small molecular systems. We therefore performed:

1. SCF calculations followed by singles and doubles configuration interaction calculations, CI(SD), as well as calculations using the coupled electron-pair approximation, CEPA1, with our quasirelativistic pseudopotentials to determine the spectroscopic constants (R_e, D_e, and ω_e) for the ground states of the neutral and singly charged silver and gold dimers, and
2. state-averaged CASSCF calculations followed by multi-reference CI(SD) calculations with our nonrelativistic and quasirelativistic pseudopotentials and with pseudopotentials already published by other groups [5, 6] to determine the spectroscopic constants (R_e, D_e, ω_e, μ_e, and $\partial\mu/\partial R$) and their sensitivity to relativistic effects for several low-lying states of ruthenium- and osmiummonohydride.

Our results are compared with those of corresponding pseudopotential calculations as well as with the published experimental data.

2. Method

The valence model Hamiltonian used in this work is (in atomic units)

$$H = -\frac{1}{2}\sum_i \Delta_i + \sum_{i,\lambda} V_\lambda(r_{i\lambda}) + \sum_{i<j}\frac{1}{r_{ij}} + \sum_{\lambda<\mu}\frac{Q_\lambda Q_\mu}{R_{\lambda\mu}}, \tag{1}$$

where $V_\lambda(r_{i\lambda})$ is a semilocal nonrelativistic or one-component quasirelativistic pseudopotential. In the case of our HF- or WB-MEFIT-PPs it has the form

$$V_\lambda(r_{i\lambda}) = -\frac{Q_\lambda}{r_{i\lambda}} + \sum_l \sum_k A_{\lambda lk}\exp(-\alpha_{\lambda lk} r_{i\lambda}^2) P_{\lambda l}, \tag{2}$$

whereas the pseudopotentials (or relativistic effective core potentials) of Hay and Wadt (denoted hereafter as HW-RECP, [5]) and of LaJohn *et al.* (denoted hereafter as LC-RECP, [6]) may be written in a slightly different form:

$$V_\lambda(r_{i\lambda}) = -\frac{Q_\lambda}{r_{i\lambda}} + \sum_k A_{\lambda Lk} r_{i\lambda}^{n_{\lambda Lk}-2}\exp(-\alpha_{\lambda Lk} r_{i\lambda}^2) + \sum_l \sum_k A_{\lambda lk} r_{i\lambda}^{n_{\lambda lk}-2}\exp(-\alpha_{\lambda lk} r_{i\lambda}^2) P_{\lambda l}, \tag{3}$$

with

$$P_{\lambda l} = \sum_{m_l} |\lambda l m_l\rangle\langle\lambda l m_l|.$$

i and j are electron indices, λ and μ are core indices; Q_λ denotes the charge of the core λ, and $P_{\lambda l}$ is the projection operator onto the Hilbert subspace with angular symmetry l with respect to core λ. $L = l_{\max} + 1$, where $l_{\max}$ is the highest angular quantum number occurring in the core.

The parameters of our HF- and WB-MEFIT-PPs, i.e., the coefficients $A_{\lambda lk}$ and the exponential parameters $\alpha_{\lambda lk}$ (cf. Eq. 2), were adjusted to HF and WB *ab initio* total valence energies of several low-lying states of the neutral atoms and

the positively charged ions, respectively, in a least squares fit (multi-electron-fit, MEFIT). More details about this fitting procedure are given in [4]. In contrast to our method, the parameters of the HW- and LC-RECPs, i.e., the coefficients $A_{\lambda Lk}$, $A_{\lambda lk}$ and the exponential parameters $n_{\lambda Lk}$, $n_{\lambda lk}$, $\alpha_{\lambda Lk}$, $\alpha_{\lambda lk}$ (cf. Eq. 3), were adjusted to orbitals and orbital energies of a single atomic reference configuration. In view of the different fitting procedures, a comparison of the resulting pseudopotentials in molecular applications seemed to be worthwhile.

The results presented in this work for the dimer molecules of noble metals and their corresponding singly charged ions were determined from SCF and subsequent CI(SD) as well as CEPA1 calculations with up to 151000 configurations. State-averaged CASSCF calculations and MRCI(SD) calculations were performed for several low-lying quartet and sextet states of the monohydrides of Ru and Os. The state averaging allowed the equivalence restricted treatment of the π orbitals of Π and Φ states and of the δ orbitals of Δ states in the CASSCF calculations, which were carried out in the point group C_{2v}. Single and double excitations were allowed from all CASSCF configurations in the MRCI(SD) calculations. The CASSCF calculations for the hydride molecules included up to 120 configurations while the MRCI(SD) calculations included between 580 000 and 770 000 configurations for the quartet states and between 96 000 and 170 000 configurations for the sextet states. The active space, taken into account for the CASSCF calculations and for the correlation treatment, was formed by the molecular orbitals from the atomic nd and $(n+1)s$ orbitals ($n = 4$ for Ru and Ag, $n = 5$ for Os and Au) and, for the hydrides, the hydrogen $1s$ orbital. The contribution of quadruple excitations was estimated by the size-consistency correction of Langhoff and Davidson ($+Q$) [7].

For Ag we used the WB-MEFIT-PP together with the optimized $(8s7p6d)/[6s5p4d]$ GTO valence basis set [4] and two f functions. The f exponents (2.6 and 0.75) were taken from [8]. For the calculations on dimeric gold systems the WB-MEFIT-PP was used with the optimized $(8s7p6d)/[6s5p3d]$ GTO valence basis set [4], augmented with two f functions (f exponents 2.0785 and 0.6). For Ru we used the HF- and WB-MEFIT-PPs together with the corresponding optimized $(8s7p6d)/[6s5p3d]$ GTO basis sets [4] and, on the other side, the HW- and LC-RECPs together with their corresponding uncontracted optimized $(5s5p4d)$ GTO valence basis sets [5, 6]. All these basis sets were augmented by a single f function, the exponent of which was chosen to be 3.0. In MRCI(SD) calculations of the type mentioned above, employing our WB-MEFIT-PP and the corresponding basis set, the ionization potential for Ru $4d^7\ 5s^1\ {}^5F$ to Ru^+ $4d^7\ {}^4F$ was calculated to be 6.73 eV, while the spin-orbit averaged experimental value is 7.37 eV [9]. For Os the HF- and WB-MEFIT-PPs were used together with the optimized $(8s7p6d)/[6s5p3d]$ GTO valence basis sets [4]. The HW-RECP for Os was used together with its uncontracted optimized $(5s5p3d)$ GTO valence basis set [5]. As in the case of Ru, one f function (f exponent 3.0) was added to all the above-mentioned basis sets for Os. With our WB-MEFIT-PP and the corresponding basis set we calculated an ionization potential for Os $5d^6\ 6s^2\ {}^5D$ to Os^+ $6s^1\ {}^6D$ of 7.57 eV at the MRCI(SD) level, while the spin-orbit averaged experimental value is 8.77 eV [9]. The differences between calculated and experimental values for the Ru and the Os ionization potentials may in part be explained by the size of our basis set, which may lead to inaccuracies in the description of the intra- and intershell correlation, while another part thereof is probably due to the omission of higher-order correlation effects. For H an extended $(10s6p1d)/[8s5p1d]$ GTO basis set was used. This basis set was built

up from an (8*s*)/[6*s*] basis set [10] to which two diffuse *s* functions (*s* exponents 0.025 and 0.01), five *p* functions (with *p* exponents 1.0, 0.3, 0.1, 0.03, and 0.01), and one *d* function (*d* exponent 0.6) were added. This large basis for H was tested for its electron affinity in CI(SD) calculations [11]: we found 0.735 eV, compared with the best calculated value of 0.7542 eV [12]. Therefore, the basis set for hydrogen should be able to yield an accurate description of the negatively polarized hydrogen atom that has been found in all examined states of the TM hydride molecules.

The asymptotic total valence energies for the lowest states of all systems considered together with the dissociation energies are given in Tables 1, 2 and 5, 6 respectively. The lowest asymptotic states of the noble metal dimers are composed of the $d^{10}\ s^1\ ^2S$ states of the neutral atoms and the $d^{10}\ ^1S$ and $d^{10}\ s^2\ ^1S$ states of the singly charged ions, respectively. For all ruthenium pseudopotentials and the nonrelativistic osmium HF-MEFIT-PP, the metal atom ^5F state of the d^7s^1 configuration, together with H $1s^1\ ^2S$, gives the lowest asymptotic total valence energy. However, in the case of the osmium WB-MEFIT-PP and HW-RECP, the lowest asymptotic total valence energy is obtained from the ^5D state of the d^6s^2 configuration of the metal atom.

All calculations were carried out with the program package MOLPRO [11]. The calculations were intended to give higher accuracy than that obtained in previous work, but to demonstrate the reliability of the nonrelativistic and quasirelativistic energy-adjusted *ab initio* pseudopotentials that we published recently. New information on the electronic structure of the OsH molecule is presented.

3. Results and discussion

3.1. Ag_2, Ag_2^+, Ag_2^- *and* Au_2, Au_2^+, Au_2^-

Theoretical investigations of the silver and gold dimers were one of the earliest applications of relativistically corrected pseudopotentials (RPP); the molecular ground states are rather simple (i.e. Σ states), spin-orbit coupling is negligible, and the importance of relativistic effects on the molecular properties can easily be demonstrated (cf., e.g., [13, 14]). Since there has been and still is great experimental interest in silver and gold clusters, most of the spectroscopic parameters for the dimeric species are available from cluster experiments. Therefore silver and gold dimers as well as their singly charged ions are suitable test molecules for which theoretical results may be compared with experimental data.

First, we wish to draw the attention to some previous RPP calculations for the neutral dimers ($X\ ^1\Sigma_g^+$ state), the positively charged dimers ($X\ ^2\Sigma_g^+$ state), and the negatively charged dimers ($X\ ^2\Sigma_u^+$ state) published in the last few years. These calculations differ from our approach in the derivation and form of the RPPs, the basis sets used and the methods for treating electron correlation. In the following paragraph we briefly characterize these calculations, selected results of which are compiled in Tables 1–3 together with the results of the present work and experimental data. Martin [8, 15] pointed out the significant improvements in the theoretical spectroscopic constants of Ag and Ag_2 when correlation is accounted for with inclusion of *f* functions in the basis set. He used the 11-electron HW-RECP [5] with a (5*s*5*p*4*d*2*f*)/[3*s*3*p*2*d*2*f*] basis set and treated

Table 1. Spectroscopic constants (R_e, D_e, ω_e) and asymptotic total valence energies for the neutral and singly charged silver dimers

Species	Method	R_e a_0	D_e eV	ω_e cm^{-1}	$E(R = 200\ a_0)$ au $-291+$
Ag_2	SCF	5.110	0.47	149	−1.167638
	CI(SD)	4.899	1.00	176	−1.767776
	CI(SD) + Q	4.867	1.20	180	−1.827255
	CEPA1	4.877	1.36	176	−1.838406
	MP4(SDQ) [8]	4.818	1.48	179	
	CPF [17]	4.885	1.48	178	
	MCPF [19]	5.023	1.34	162	
	LMRCI [24]	4.878	1.43	198	
	exp	4.69[b]	1.68[a]	192[a]	
Ag_2^+	SCF	5.715	1.18	87	−0.934647
	CI(SD)	5.363	1.33	108	−1.513761
	CI(SD) + Q	5.296	1.39	114	−1.567679
	CEPA1	5.274	1.41	116	−1.575203
	exp	—	1.66[c]	—	
Ag_2^-	SCF	5.478	0.56	100	−1.171799
	CI(SD)	5.178	0.93	123	−1.787266
	CI(SD) + Q	5.139	1.06	128	−1.853786
	CEPA1	5.144	1.16	127	−1.877349
	MCPF [19]	5.318	1.12	118	
	exp	—	1.39[d]	—	

[a] From [25]
[b] Estimated value from [18]
[c] Ref. 26 in [21]
[d] Ref. 4 in [19]

correlation by Møller–Plesset perturbation theory up to fourth order (MP4). The use of the more accurate 19-electron HW-RECP led to an increase of only 0.04 a_0 in the bond length at the SCF level, in agreement with a corresponding value of 0.06 a_0 found by Ross and Ermler [16]. However, larger differences may arise when correlation is taken into account: in a similar study on Au_2 Walch et al. [17] reported a bond length enlarged by 0.15 a_0 for the HW-RECPs at the coupled pair functional (CPF) level, indicating the superiority of 19-electron pseudopotentials over 11-electron ones. Walch et al. determined bond distances, dissociation energies and vibrational frequencies for the neutral silver and gold dimers from CPF calculations using the 19-electron HW-RECPs with a [$5s4p3d5f$] valence basis set for Ag and a [$4s3p3d2f$] valence basis set for Au, respectively. Another important result from the work of Martin [8], Hay and Martin [15] and Walch et al. [17] is, that the recommended experimental value of 4.69 a_0 for the bond distance of Ag_2, which was determined with the empirical Morse–Clark formula ($R_e^3\omega_e = \text{const.}$) from the spectroscopic constants of Cu_2

Table 2. Spectroscopic constants (R_e, D_e, ω_e) and asymptotic total valence energies for the neutral and singly charged gold dimers

Species	Methods	R_e a_0	D_e eV	ω_e cm^{-1}	$E(R = 200\ a_0)$ au $-269+$
Au_2	SCF	4.942	0.81	155	−0.565993
	CI(SD)	4.809	1.47	174	−1.089500
	CI(SD) + Q	4.794	1.67	176	−1.146012
	CEPA1	4.799	1.82	173	−1.157665
	CPF [17]	4.78	1.97	179	
	MCPF [19]	4.842	1.87	172	
	CEPA1 [23]	4.800	1.85	170	
	exp	4.67[a]	2.30[a]	191[a]	
Au_2^+	SCF	5.372	1.30	95	−0.284306
	CI(SD)	5.130	1.59	120	−0.777895
	CI(SD) + Q	5.089	1.69	124	−0.827190
	CEPA1	5.069	1.79	130	−0.835122
	CEPA1 [23]	5.097	1.75	125	
Au_2^-	SCF	5.237	0.85	105	−0.589874
	CI(SD)	5.067	1.33	126	−1.139338
	CI(SD) + Q	5.049	1.46	128	−1.205292
	CEPA1	5.042	1.58	130	−1.227505
	MCPF [19]	5.094	1.61	125	
	CEPA1 [23]	5.032	1.63	131	
	exp	4.879[b]	1.94[b]	149[b]	

[a] From [25]
[b] Ref. 4 in [19]

and Au_2 [18], may be too short. The electron affinities of Ag, Au, Ag_2, and Au_2 were examined by Bauschlicher et al. [19], who used the 19-electron HW-RECPs together with $(6s6p4d3f)/[5s4p4d1f]$ valence basis sets for Ag and Au in calculations with the modified CPF method (MCPF [20]). The corresponding ionization potentials have been studied by Balasubramanian and Feng [21] in CASSCF/MRCI calculations using the 11-electron pseudopotentials of LaJohn et al. [6] and Ermler and Christiansen [22] together with $(3s3p3d)$ valence basis sets. Schwerdtfeger et al. [23] recently treated Au_2 and its singly charged ions. They used a RPP, which was adjusted to spin-orbit averaged Dirac–Fock (DF) energies in a procedure analogous to our WB-MEFIT-PP, together with a $(8s6p5d1f)/[7s3p4d1f]$ valence basis set. For correlation treatment they used the CI(SD) and the CEPA1 method. They reported spectroscopic constants, ionization potentials and electron affinities. In a recent study on Ag_3 Ramirez-Solis et al. [24] reported values for the spectroscopic constants R_e, D_e, and ω_e for the silver dimer from MRCI calculations with localized molecular orbitals (LMRCI), using an 11-electron RECP with a $[3s2p3d1f]$ basis set for Ag.

Table 3. Ionization potentials and electron affinities (in eV) for the silver and gold atoms and neutral dimers

Species	Method	IP eV	EA eV
Ag	SCF	6.34	0.11
	CI(SD)	7.01	0.67
	CI(SD) + Q	7.13	0.88
	CEPA1	7.16	1.06
	MP4(SDQ) [8]	7.22	—
	MCPF [19]	—	0.97
	CASSCF/MRCI(SD) [21]	6.73	—
	exp	7.57[a]	1.30[b]
Ag_2	SCF	5.64	0.20
	CI(SD)	6.58	0.46
	CI(SD) + Q	6.88	0.58
	CEPA1	7.11	0.86
	MCPF [19]	—	0.75
	CASSCF/MRCI(SD) [21]	6.7	—
	exp	7.56[c]	1.03[d]
Au	SCF	7.67	0.65
	CI(SD)	8.81	1.52
	CI(SD) + Q	8.75	1.78
	CEPA1	8.78	1.90
	MCPF [19]	—	1.86
	CASSCF/MRCI(SD) [21]	8.57	—
	exp	9.22[a]	2.31[b]
Au_2	SCF	7.18	0.69
	CI(SD)	8.35	1.21
	CI(SD) + Q	8.66	1.40
	CEPA1	8.81	1.66
	MCPF [19]	—	1.59
	CASSCF/MRCI(SD) [21]	8.78	—
	CEPA1 [23]	8.55	1.54
	exp	—	1.94[d]

[a] From [9]
[b] From [12]
[c] Ref. 26 in [21]
[d] Ref. 4 in [19]

The spectroscopic constants R_e, D_e, and ω_e for the dimeric silver and gold species are collected in Tables 1 and 2. We shall consider the bond lengths first. A comparison of calculated values with experimental data is possible for Ag_2, Au_2, and Au_2^-. Our values correctly reflect the differential bond length increase from the neutral to the negatively charged species ($\Delta R_e = 0.24\, a_0$ (CEPA1) vs. $\Delta R_e = 0.21\, a_0$ (exp.) for Au_2 and Au_2^-) but they are systematically too large in

the absolute value (by ca. 0.19 a_0 for Ag_2 and 0.13 a_0 for Au_2 at the CEPA1 level). Much better is the agreement of our CEPA1 values with other theoretical values obtained at similar levels of correlation treatment (CPF [17], CEPA1 [23], LMRCI [24]); here the differences are smaller than 0.03 a_0. The MCPF results [19] are systematically larger (by ca. 0.15 a_0 for Ag_2 and Ag_2^-, and by ca. 0.05 a_0 for Au_2 and Au_2^-); part of this discrepancy may be due to the smaller basis set used in [19]. The MP4(SDQ) calculation [8], on the other hand, yields a bond length for Ag_2 which is smaller than our CEPA1 value by 0.07 a_0, probably reflecting the tendency to overestimate correlation effects with MP4. Thus, the level of valence correlation treatment and the size of the valence basis set seem to have a much larger influence on the bond lengths considered than do the pseudopotentials: various 19-electron pseudopotentials lead to almost the same results when valence interaction is treated with similar accuracy.

Turning now to vibrational frequencies, a similar picture evolves. Our overestimation of bond lengths leads to an underestimate for the vibrational frequencies compared with experiment (by 15–20 cm^{-1} (CEPA1) for Ag_2, Au_2, and Au_2^-). On the other hand, the comparison with other CEPA1 [23] and CPF [17] calculations gives much better agreement (differences are smaller than 6 cm^{-1}).

For the dissociation energies, finally, the situation is a bit more complicated. Our calculated values only roughly describe the differential increase of D_e from Ag_2 to Au_2 ($\Delta D_e = 0.46$ eV (CEPA1) vs. $\Delta D_e = 0.62$ eV (exp.)), and the differential effects within a given elemental species are reproduced within 0.15 eV on the CEPA1 level: we get a small but incorrect increase in D_e from Ag_2 to Ag_2^+ (by 0.05 eV (CEPA1) vs. −0.02 eV (exp.)) and too small a decrease from Ag_2 to Ag_2^- (by 0.20 eV (CEPA1) vs. 0.29 eV (exp.)) and from Au_2 to Au_2^- (by 0.24 eV (CEPA1) vs. 0.36 eV (exp.)). The reason is not entirely clear, but is certainly connected with the fact that both the atomic ionization potentials and electron affinities are too small in our approach (cf. the discussion below). The agreement of our CEPA1 D_e values with other theoretical results is good. The deviations are smaller than 0.05 eV both for the silver and gold compounds compared with the MCPF [19] and CEPA1 results [23] respectively. However, the agreement with the CPF results [17] is poorer, with deviations of up to 0.15 eV. Thus, while our CEPA1 R_e values agree well with those from the CPF approach of [17], for our CEPA1 D_e values the agreement is better with the MCPF results [19].

Ionization potentials (IP) and electron affinities (EA) for the silver and gold atoms and dimers are given in Table 3, together with experimental and other theoretical results. As already stated, all of our CEPA1 values are all smaller than experiment by up to 0.45 eV for the atomic and dimeric ionization potentials and electron affinities, with the largest error being for the Ag_2 IP. While the error in the IP increases by 0.04 eV from atomic to dimeric silver, the error for the dimeric EA is only half in the atomic EA. Apparently, our basis sets are too limited to cover $s-d$ intershell correlation effects fully. However, none of the other theoretical values [8, 17, 19, 21, 23] performs any better. Again, the problem is not due to the pseudopotential used but to inaccuracies in the treatment of valence interactions.

3.2. RuH *and* OsH

As a further test of our energy-adjusted *ab initio* pseudopotentials, theoretical studies on the monohydrides of ruthenium and osmium, RuH and OsH, were

performed. Although these molecules may be regarded as rather primitive ones because of the simple bonding between the hydrogen atom and the TM atom, the two TM atoms, being in the middle of their rows, show several low-lying states with rather high spin-multiplicities and therefore are more difficult to handle than, e.g., the noble metal atoms Ag and Au.

Before proceeding to present our results on RuH and OsH we wish to give a short review of the experimental and theoretical work on these two molecules done by other groups. To our knowledge, there is still no experimental spectroscopic data for these hydrides. Only RuH has been investigated in an experimental study: by Tolbert and Beauchamp [26] using a molecular-beam technique. They found a dissociation energy of 2.4 ± 0.2 eV, noted by them as a lower bound to the real value, and assigned the ground state of RuH to be a $^4\Phi$ state by comparing their experimental results with theoretical calculations by Krauss and Stevens [27]. This ground state had been predicted previously by Squires [28] from an analysis of thermochemical data for other TM hydrides. On the theoretical side, several authors worked on RuH. Krauss and Stevens [27] performed complete active space self-consistent field (CASSCF) calculations of the lowest $^2\Phi$, $^4\Delta$, and $^6\Delta$ states using a Ru 16-electron RPP (averaged relativistic effective potential, AREP) and STO basis sets of augmented DZ quality for Ru and H, and found the $^4\Phi$ state to be the lowest state. Langhoff et al. [29] treated all second row TM monohydrides with TM atom RPPs (relativistic effective core potentials, RECP) representing the $M^{(Z-28)+}$ cores. For RuH they used a generally contracted $(6s6p5d4f)/[5s4p5d4f]$ Ru valence basis set and a $(7s4p)/[4s3p]$ H basis set. They reported spectroscopic constants for the lowest $^4\Phi$, $^4\Delta$, and $^6\Delta$ states of RuH and they also found the $^4\Phi$ state to be the lowest state. The most detailed investigation of RuH yet published was made by Balasubramanian and Wang [30]. They performed state averaged CASSCF, first order CI, and MRCI(SD) calculations for 21 electronic sextet, quartet, and doublet states of RuH with an 8-electron RPP, a $[4s3p4d1f]$ valence basis set for Ru and a $[3s1p]$ basis set for H. Among these states they found a $^4\Sigma^-$ state to be the ground state, while the $^4\Phi$ state with term energy $T_e = 2848\ \text{cm}^{-1}$ turned out to be nearly degenerate with a $^4\Pi$ state with $T_e = 2802\ \text{cm}^{-1}$. This study was the first which did not predict a $^4\Phi$ ground state but rather a $^4\Sigma^-$ ground state for RuH, for which a dissociation energy of 2.89 eV was calculated at the first-order CI level. This value was then corrected for higher-order correlation effects and basis set extensions to 3.1 ± 0.2 eV. Unfortunately, parameters for the RPP employed in [30] are not given, which limits the comparison with our data. We performed CASSCF and MRCI(SD) calculations to provide further hints for the theoretical side to the ground state of RuH and to compare the behaviour of the available 16-electron pseudopotentials for ruthenium in a molecular environment. In this work we applied the published RPPs for Ru from Hay and Wadt [5] and from LaJohn et al. [6] as well as our HF-MEFIT-PP and WB-MEFIT-PP [4] to investigate seven low-lying electronic sextet and quartet states of RuH: $^4\Sigma^-$, $^4\Pi$, $^4\Delta$, $^4\Phi$, $^6\Sigma^+$, $^6\Pi$, and $^6\Delta$. All three relativistically corrected pseudopotentials yield a qualitatively similar overall picture with only minor differences. Both the nonrelativistic HF-MEFIT-PP and the RPPs give the $^4\Sigma^-$ state as ground state.

Neither experimental nor theoretical data are known for OsH. As in the case of RuH we performed calculations of the same quality for the same seven low-lying states of OsH with the available 16-electron pseudopotentials for osmium. We compare in this work the RPP for Os by Hay and Wadt [5] (which

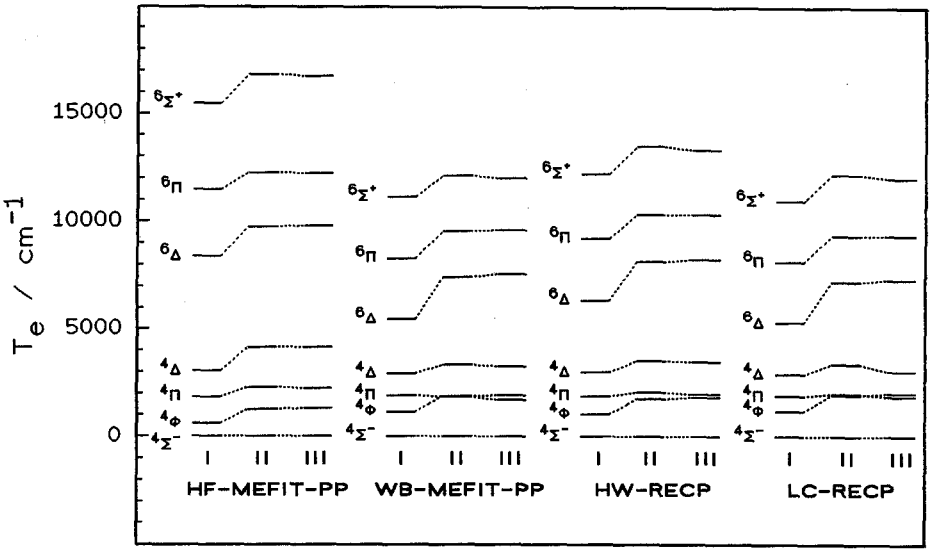

Fig. 1. Term energies for RuH from CASSCF (I), MRCI(SD) (II), and MRCI(SD) + Q (III) calculations

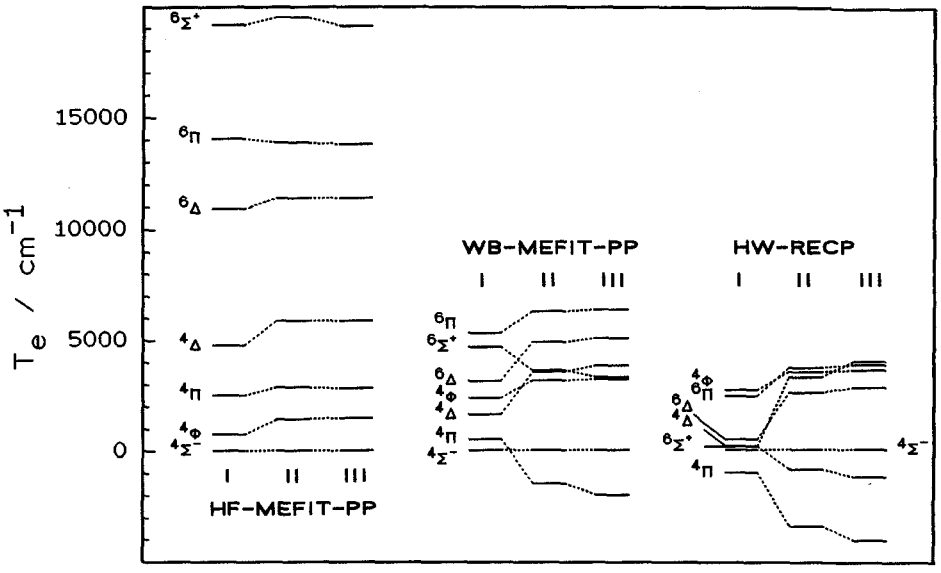

Fig. 2. Term energies for OsH from CASSCF (I), MRCI(SD) (II), and MRCI(SD) + Q (III) calculations

is the only one published in literature) with our WB-MEFIT-PP and also give the results obtained with our nonrelativistic HF-MEFIT PP. The HF-MEFIT-PPs for Os and Ru give qualitatively similar pictures of the molecular structure of the hydrides (cf., e.g., the term energies shown in Figs. 1 and 2), which reflects that both atoms have the same nonrelativistic ground state configuration.

However, the two relativistically corrected osmium pseudopotentials show larger differences compared with both the nonrelativistic case and with each other in their predictions of the molecular electronic structure of OsH than do the ruthenium pseudopotentials in the case of RuH, although both RPPs for Os yield a $^4\Pi$ state as ground state for OsH.

The leading molecular electron configurations for the above-mentioned states of the monohydrides are given in Table 4, showing the molecular orbitals which stem from the hydrogen 1*s* orbital and the TM atom *nd* and $(n+1)s$ orbitals ($n = 4$ for Ru, $n = 5$ for Os). State designations in the real molecular point group $C_{\infty v}$ and, in parentheses, in the point group C_{2v} used in our CASSCF and MRCI(SD) calculations [11] are also given. We used the CASSCF natural orbitals for the MRCI(SD) calculations. For those states which need state-averaging for a proper description in the CASSCF calculation the MRCI(SD) calculations were performed in the first irreducible representation given in parentheses in Table 4, e.g., B_1 for the Π states. As a measure of the contribution of the leading electron configuration(s) to the desired molecular state, the last four columns of this table give the sum of the squares of the CI coefficients for the contributing determinants in C_{2v}, calculated at the equilibrium distance with

Table 4. Leading molecular electron configurations for the seven examined states of ruthenium- and osmiummonohydride, RuH and OsH, and sums of the squares of the CI coefficients for the contributing determinants from MRCI(SD) calculations at the equilibrium distance, determined with various pseudopotentials

Electronic state	Leading electron configurations	Σc_i^2			
		MEFIT-PP		RECP	
		HF	WB	HW	LC
1. RuH					
$^4\Sigma^-$ ($^4A_2$)	$\sigma^2\sigma^1\pi^4\delta^2$	0.82	0.83	0.83	0.84
$^4\Pi$ ($^4B_1$, $^4B_2$)	$\sigma^2\sigma^2\pi^3\delta^2$	0.31	0.44	0.40	0.44
	$\sigma^2\sigma^1\pi^3\delta^3$	0.60	0.47	0.52	0.48
$^4\Delta$ ($^4A_1$, $^4A_2$)	$\sigma^2\sigma^2\pi^2\delta^3$	0.92	0.91	0.92	0.91
$^4\Phi$ ($^4B_1$, $^4B_2$)	$\sigma^2\sigma^1\pi^3\delta^3$	0.92	0.92	0.92	0.92
$^6\Sigma^+$ ($^6A_1$)	$\sigma^2\sigma^2\sigma^1\pi^2\delta^2$	0.93	0.93	0.93	0.93
$^6\Pi$ ($^6B_1$, $^6B_2$)	$\sigma^2\sigma^1\sigma^1\pi^3\delta^2$	0.93	0.93	0.94	0.94
	$\sigma^1\sigma^1\sigma^1\pi^3\delta^3$	0.01	—[a]	0.01	—[a]
$^6\Delta$ ($^6A_1$, $^6A_2$)	$\sigma^2\sigma^1\sigma^1\pi^2\delta^3$	0.94	0.94	0.94	0.94
2. OsH					
$^4\Sigma^-$ ($^4A_2$)	$\sigma^2\sigma^1\pi^4\delta^2$	0.83	0.87	0.87	
$^4\Pi$ ($^4B_1$, $^4B_2$)	$\sigma^2\sigma^2\pi^3\delta^2$	0.24	0.78	0.83	
	$\sigma^2\sigma^1\pi^3\delta^3$	0.68	0.12	0.06	
$^4\Delta$ ($^4A_1$, $^4A_2$)	$\sigma^2\sigma^2\pi^2\delta^3$	0.92	0.91	0.93	
$^4\Phi$ ($^4B_1$, $^4B_2$)	$\sigma^2\sigma^1\pi^3\delta^3$	0.93	0.92	0.92	
$^6\Sigma^+$ ($^6A_1$)	$\sigma^2\sigma^2\sigma^1\pi^2\delta^2$	0.93	0.92	0.92	
$^6\Pi$ ($^6B_1$, $^6B_2$)	$\sigma^2\sigma^1\sigma^1\pi^3\delta^2$	0.93	0.94	0.94	
	$\sigma^1\sigma^1\sigma^1\pi^3\delta^3$	0.01	—[a]	—[a]	
$^6\Delta$ ($^6A_1$, $^6A_2$)	$\sigma^2\sigma^1\sigma^1\pi^2\delta^3$	0.94	0.94	0.94	

[a] c_i's smaller than 0.05

the various pseudopotentials employed. With the exception of the $^4\Pi$ states, only a single configuration is sufficient for an approximate description of all states considered. The RuH $^4\Pi$ state is constituted mainly from two configurations, which contribute almost equally in the calculations with the RPPs. This also reflects the near-degeneracy of the $^4\Pi$ and the $^4\Phi$ states, which was found in the case of RuH with these pseudopotentials (cf. discussion below, Table 5 and Fig. 1). In the case of OsH the $^4\Pi$ state is also mainly built up from the two configurations, but these no longer contribute to nearly the same extent. The calculations with the osmium HF-MEFIT-PP led to a $^4\Phi$ state which is lower in energy than the $^4\Pi$ state, as in the case of RuH, but this sequence is inverted, when the RPPs are used. Now the $^4\Pi$ state becomes the ground state of OsH (cf. discussion below, Table 6 and Fig. 2). This inversion between the calculations performed with the osmium HF-MEFIT-PP and the RPPs, respectively, as well as the larger separation between them is reflected in the values given in Table 4. For the comparable sextet states, $^6\Pi$ and $^6\Phi$, the situation is quite different and much less complicated: the $^6\Pi$ state is the lower one in the CASSCF and MRCI(SD) calculations with any pseudopotential, leaving the $^6\Phi$ state so high that it was not examined further in this work.

In Table 5 the calculated spectroscopic constants for the investigated electronic states of RuH are collected. The dissociation energies D_e were calculated relative to the asymptotic total valence energies which can be found at the bottom of Table 5 (see also Sect. 2). The molecular term energies T_e and their change with the method and the PP employed, given relative to the $^4\Sigma^-$ state, are shown in Fig. 1. The term sequence found for RuH is the same for nearly all levels of theoretical treatment. The $^4\Sigma^-$ state is the lowest state and can therefore be regarded as the theoretically predicted ground state. All sextet states examined lie above the quartet states we considered. A term inversion with respect to the term sequence obtained from the CASSCF calculations was found only for the excited $^4\Phi$ and $^4\Pi$ states in MRCI(SD) calculations with the WB-MEFIT-PP and, when the size-consistency correction was included, with the WB-MEFIT-PP and the LC-RECP; it was not found for the HW-RECP, indicating certain differences in the quality of the pseudopotentials and/or the basis sets. The overall picture for the electronic structure of RuH obtained with the different RPPs is roughly consistent, although the best agreement was obtained between the results from the calculations with the WB-MEFIT-PP and the LC-RECP, a behaviour which is also found in atomic calculations [4] (cf. also discussion below). This inversion of the excited $^4\Phi$ and $^4\Pi$ states was also found in MRCI(SD) calculations [30] (CASSCF term energy values are not reported); however, the absolute values for the term energies for the states considered in our work show significant differences from those reported in [30]. In general the quartet states are systematically higher, while the sextet states are systematically lower are (in most cases, the differences are between 1000 cm^{-1} and 2000 cm^{-1}). The reason for this different picture may lie in shortcomings of the 8-electron RPP employed in [30] and in the use of rather small basis sets.

For the bond distances R_e of the various states the expected decrease was found when correlation was taken into account. This leads to rather similar bond distances for the nearly-degenerate excited $^4\Pi$ and $^4\Phi$ states. The bond distance sequence among the states examined, as it results from MRCI(SD) calculations, can also be found in [30], although their bond distances are slightly shorter than ours with differences of up to 0.09 a_0.

The polarity of the seven states, given by the absolute value of the dipole moment μ_e, changes in the same way for all PPs and methods. The most polar state is the $^4\Delta$ state—the only one which describes the RuH molecule as Ru^+-H^- according to the orbital configuration in Table 4. All sextet states show a much lower polarity than the quartet states, reflecting the occupation of an antibonding σ molecular orbital. In all but one case the hydrogen atom was found to be the negatively polarized part of the RuH molecule. The only exception is the dipole moment for the $^6\Delta$ state from MRCI(SD) calculations with the HF-MEFIT-PP.

There is good agreement with the data from [30] for the dipole moments of the seven states examined here. The values reported in earlier works for the bond distances, dissociation energies, and dipole moments of the $^4\Phi$, $^4\Delta$, and $^6\Delta$ states of RuH [27, 29] are in qualitative agreement with our results, although, due to the different methods and PPs employed, certain differences in the absolute values are found: the bond lengths reported by Krauss and Stevens (AREP, CASSCF [27]) are significantly shorter than ours (the differences from our CASSCF values are between 0.1 a_0 and 0.2 a_0), although the dissociation energies (which can be calculated from the reported data only for the Δ states) reveal a different picture, with their value for the $^4\Delta$ state being 0.03 eV larger than our CASSCF value, but that for the $^6\Delta$ state being 0.6 eV smaller. Langhoff et al. (RECP, CI(SD) and MCPF [29]) obtained bond lengths which are significantly longer than ours (0.08 a_0 longer than MRCI(SD) and MRCI(SD) + Q values) and dissociation energies which are slightly lower than our values (0.03–0.09 eV with respect to our MRCI(SD) and MRCI(SD) + Q values.

A comparison of the data obtained with the HF-MEFIT-PP with those obtained with the RPPs shows the expected relativistic effects: bond distances shorten and the dissociation energy increases in all seven of the states of RuH that we examined, and the vibrational frequencies also increase. These effects are of similar magnitude for the LC-RECP [6] and the WB-MEFIT-PP [4]. These two RPPs also show quite similar values for the spectroscopic parameters, which indicates a certain convergence in the description of the molecular electron structure, while the results obtained with the HW-RECP [5] lie between the results obtained with the HF-MEFIT-PP and the other two RPPs. Another point to be mentioned is the large change in the bond distance for the $^4\Delta$ state between the CASSCF calculations with the HF-MEFIT-PP and WB-MEFIT-PP. This large relativistic effect on R_e may be interpreted as a differential relativistic effect on the metal valence orbitals. Another relativistic effect is the decrease of the polarity of all but the $^6\Pi$ and $^6\Delta$ states, for which the polarity is increased. The polarity change, compared with the HF-MEFIT-PP for a given state is of similar magnitude for all three RPPs. However, none of these RPPs performs better for the dipole moment which indicates that difficulties in the calculation of properties that depend sensitively on changes of the wavefunction still remain.

The calculations on OsH were performed with the HF-MEFIT-PP, the WB-MEFIT-PP [4], and with the HW-RECP [5] using the corresponding optimized valence basis sets. In the nonrelativistic case, i.e., when the HF-MEFIT-PP is used, the ground state of the osmium atom is $5d^7\ 6s^1\ ^5F$ while the $5d^6\ 6s^2\ ^5D$ state is calculated to be the ground state in the quasirelativistic case, i.e., when one of the two RPPs is used [4], reflecting the influence of relativistic effects in the atom. The dissociation energies D_e for the seven states considered (which can be found, together with other calculated spectroscopic parameters, in Table 6) were calculated relative to the asymptotic total valence energies in the

Table 5. Spectroscopic parameters and other properties for the low-lying states of RuH

State and property[a]		HF-MEFIT-PP		WB-MEFIT-PP			HW-RECP			LC-RECP		
		CASSCF	MRCI(SD)	MRCI(SD)+Q	CASSCF	MRCI(SD)	MRCI(SD)+Q	CASSCF	MRCI(SD)	MRCI(SD)+Q	CASSCF	MRCI(SD)	MRCI(SD)+Q
$^4\Sigma^-$	R_e	3.222	3.012	3.001	3.140	2.963	2.954	3.165	2.988	2.977	3.146	2.973	2.963
	D_e	1.79	2.77	2.85	1.91	2.92	3.01	1.88	2.84	2.93	1.92	2.91	3.00
	T_e	0	0	0	0	0	0	0	0	0	0	0	0
	ω_e	1463	1829	1852	1647	1995	2019	1614	1917	1948	1656	1961	1983
	μ_e	−3.557	−3.100		−3.038	−2.726		−3.123	−2.844		−3.111	−2.858	
	$\partial\mu/\partial R$	−3.63	−3.39		−3.02	−2.75		−3.15	−3.00		−3.09	−2.94	
$^4\Pi$	R_e	3.366	3.127	3.110	3.242	3.033	3.017	3.276	3.073	3.057	3.250	3.054	3.038
	D_e	1.57	2.49	2.57	1.68	2.69	2.80	1.64	2.59	2.69	1.69	2.66	2.76
	T_e	1809	2271	2218	1882	1841	1697	1879	2067	1965	1888	1999	1878
	ω_e	1365	1709	1738	1532	1902	1932	1498	1815	1844	1537	1850	1877
	μ_e	−4.216	−3.730		−3.560	−3.154		−3.665	−3.321		−3.627	−3.296	
	$\partial\mu/\partial R$	−2.73	−2.98		−2.51	−2.63		−2.58	−2.79		−2.58	−2.79	
$^4\Delta$	R_e	3.480	3.229	3.214	3.330	3.121	3.115	3.343	3.151	3.143	3.309	3.135	3.128
	D_e	1.41	2.26	2.34	1.55	2.51	2.60	1.51	2.41	2.50	1.56	2.49	2.59
	T_e	3033	4140	4146	2914	3323	3263	2985	3530	3477	2905	3366	3046
	ω_e	1279	1647	1688	1449	1886	1930	1410	1783	1826	1453	1822	1864
	μ_e	−4.686	−4.304		−3.885	−3.554		−4.015	−3.709		−3.938	−3.656	
	$\partial\mu/\partial R$	−2.03	−2.50		−2.49	−2.61		−2.47	−2.74		−2.58	−2.77	
$^4\Phi$	R_e	3.295	3.090	3.079	3.204	3.031	3.022	3.234	3.060	3.051	3.215	3.048	3.038
	D_e	1.72	2.61	2.69	1.77	2.69	2.77	1.75	2.63	2.71	1.78	2.67	2.75
	T_e	591	1253	1302	1133	1869	1922	1027	1744	1811	1172	1936	2009
	ω_e	1385	1726	1759	1543	1887	1908	1514	1817	1838	1547	1847	1867
	μ_e	−3.950	−3.447		−3.334	−2.981		−3.446	−3.124		−3.420	−3.127	
	$\partial\mu/\partial R$	−3.74	−3.57		−3.37	−3.16		−3.44	−3.35		−3.43	−3.35	

Table 5 (continued)

$^6\Sigma^+$	R_e	3.578	3.429	3.421	3.480	3.333	3.324	3.508	3.376	3.370	3.474	3.349	3.343
	D_e	−0.13	0.69	0.78	0.53	1.42	1.52	0.36	1.17	1.28	0.56	1.40	1.51
	T_e	15462	16793	16727	11126	12111	11996	12215	13496	13342	10968	12185	12026
	ω_e	1447	1541	1534	1516	1648	1646	1491	1596	1590	1528	1640	1635
	μ_e	−1.497	−1.026		−1.258	−0.788		−1.307	−0.884		−1.228	−0.841	
	$\partial\mu/\partial R$	−3.91	−3.26		−3.87	−3.22		−3.93	−3.28		−3.79	−3.17	
$^6\Pi$	R_e	3.408	3.261	3.256	3.375	3.234	3.229	3.394	3.257	3.253	3.372	3.239	3.235
	D_e	0.37	1.25	1.33	0.89	1.74	1.81	0.73	1.56	1.65	0.91	1.75	1.84
	T_e	11474	12238	12219	8283	9558	9608	9209	10355	10338	8136	9354	9351
	ω_e	1551	1659	1658	1589	1694	1693	1573	1675	1671	1607	1706	1702
	μ_e	−0.784	−0.144		−0.884	−0.314		−0.881	−0.307		−0.864	−0.331	
	$\partial\mu/\partial R$	−4.94	−4.19		−4.77	−4.14		−4.84	−4.21		−4.68	−4.08	
$^6\Delta$	R_e	3.421	3.311	3.310	3.398	3.288	3.284	3.415	3.309	3.307	3.397	3.293	3.291
	D_e	0.75	1.56	1.63	1.24	2.00	2.07	1.09	1.83	1.91	1.26	2.01	2.09
	T_e	8372	9736	9796	5453	7424	7572	6357	8174	8261	5314	7227	7332
	ω_e	1602	1681	1675	1625	1704	1705	1620	1691	1684	1646	1720	1713
	μ_e	−0.562	0.022		−0.767	−0.250		−0.755	−0.235		−0.759	−0.271	
	$\partial\mu/\partial R$	−4.83	−4.03		−4.67	−4.10		−4.70	−4.11		−4.54	−3.99	
$E(R=200\ a_0)$													
−93+		−0.853942	−0.917661	−0.920078	−1.592668	−1.658430	−1.661158	−0.612009	−0.692469	−0.695352	−1.168357	−1.248120	−1.250918

[a] R_e in a_0; D_e in eV; T_e in cm^{-1}; ω_e in cm^{-1}; μ_e in D; $\partial\mu/\partial R$ in D/A (negative values for the dipole moment denote the polarity $M(+)-H(-)$)

Table 6. Spectroscopic parameters and other properties for the low-lying states of OsH

State and property[a]		HF-MEFIT-PP			WB-MEFIT-PP			HW-RECP		
		CASSCF	MRCI(SD)	MRCI(SD) + Q	CASSCF	MRCI(SD)	MRCI(SD) + Q	CASSCF	MRCI(SD)	MRCI(SD) + Q
$^4\Sigma^-$	R_2	3.232	3.070	3.062	3.088	2.970	2.964	3.082	2.969	2.963
	D_e	1.93	2.91	2.98	1.95	2.49	2.47	1.68	2.23	2.22
	T_e	0	0	0	0	0	0	0	0	0
	ω_e	1613	1909	1927	2014	2285	2304	2077	2303	2315
	μ_e	−3.144	−2.894		−2.138	−2.043		−2.118	−2.031	
	$\partial\mu/\partial R$	−3.46	−3.07		−1.65	−1.35		−1.54	−1.22	
$^4\Pi$	R_e	3.378	3.190	3.178	3.080	2.965	2.956	3.058	2.957	2.950
	D_e	1.62	2.55	2.63	1.88	2.67	2.72	1.80	2.66	2.73
	T_e	2509	2880	2829	511	−1503	−2017	−1031	−3454	−4128
	ω_e	1434	1736	1767	2025	2303	2327	2109	2324	2339
	μ_e	−3.866	−3.514		−1.880	−1.685		−1.525	−1.423	
	$\partial\mu/\partial R$	−3.13	−3.11		−1.57	−1.21		−1.04	−0.80	
$^4\Delta$	R_e	3.556	3.331	3.317	3.121	3.209	3.235	3.098	3.024	3.023
	D_e	1.34	2.18	2.25	1.75	2.05	2.00	1.65	1.83	1.73
	T_e	4773	5876	5871	1615	3542	3843	175	3277	3989
	ω_e	1290	1634	1671	1970	2037	2012	2041	2128	2119
	μ_e	−4.631	−4.310		−1.907	−2.082		−1.518	−1.624	
	$\partial\mu/\partial R$	−2.04	−2.49		−1.41	−1.06		−0.91	−0.94	
$^4\Phi$	R_e	3.293	3.144	3.137	3.118	3.013	3.008	3.111	3.011	3.006
	D_e	1.84	2.73	2.80	1.65	2.09	2.08	1.34	1.80	1.78
	T_e	750	1426	1477	2362	3161	3208	2703	3522	3589
	ω_e	1524	1803	1818	1969	2205	2219	2032	2239	2251
	μ_e	−3.474	−3.206		−2.087	−2.023		−1.999	−1.948	
	$\partial\mu/\partial R$	−3.69	−3.31		−1.75	−1.55		−1.58	−1.36	

Table 6 (continued)

$^6\Sigma^+$	R_e	3.654	3.518	3.511	3.356	3.265	3.262	3.296	3.218	3.216
	D_e	−0.44	0.52	0.61	1.36	2.04	2.07	1.66	2.34	2.38
	T_e	19174	19500	19110	4688	3621	3298	162	−891	−1252
	ω_e	1437	1531	1524	1737	1853	1848	1832	1936	1930
	μ_e	−1.457	−0.997		−0.692	−0.347		−0.474	−0.203	
	$\partial\mu/\partial R$	−4.06	−3.37		−3.95	−3.29		−3.67	−3.04	
$^6\Pi$	R_e	3.449	3.336	3.335	3.352	3.248	3.247	3.314	3.216	3.216
	D_e	0.19	1.18	1.27	1.29	1.71	1.69	1.37	1.77	1.75
	T_e	14061	13908	13818	5306	6298	6365	2444	3727	3838
	ω_e	1580	1668	1662	1688	1782	1774	1758	1853	1843
	μ_e	−0.395	0.070		−0.703	−0.331		−0.586	−0.296	
	$\partial\mu/\partial R$	−5.20	−4.10		−4.72	−3.90		−4.28	−3.49	
$^6\Delta$	R_e	3.474	3.394	3.395	3.396	3.313	3.311	3.362	3.281	3.281
	D_e	0.58	1.49	1.56	1.56	1.88	1.85	1.62	1.91	1.87
	T_e	10927	11428	11414	3138	4898	5054	481	2587	2811
	ω_e	1624	1675	1666	1691	1761	1753	1754	1824	1814
	μ_e	−0.231	0.178		−0.805	−0.421		−0.709	−0.386	
	$\partial\mu/\partial R$	−4.95	−3.89		−4.68	−3.98		−4.28	−3.61	
$E(R-200\,a_0)$										
$-87+$		−0.334842	−0.381089	−0.32736	−3.317048	−3.390705	−3.396777	−3.713208	−3.800168	−3.807251

[a] R_e in a_0; D_e in eV; T_e in cm^{-1}; ω_e in cm^{-1}; μ_e in D; $\partial\mu/\partial R$ in D/A (negative vaues for the dipole moment denote the polarity M(+)−H(−1))

last row of this table (see also Sect. 2). Due to the difference in the atomic ground states in the realtivistic case, results similar to those obtained for RuH could be expected only for the calculations with the HF-MEFIT-PP for Os. Hence, the sequence of the bond distances and the term sequence are the same as in the case of RuH for the similar states. The calculations which were performed with the two RPPs show quite different results, mainly due to the different atomic ground state for Os. With both of these pseudopotentials the quartet states show shorter bond distances compared with those of the sextet states and both lead to a $^4\Pi$ ground state for OsH. A point to be mentioned here is the unexpected bond length increase found at the MRCI(SD) level for the $^4\Delta$ state when the WB-MEFIT-PP is used. This increase was not found for either the $^4\Delta$ state of RuH or for any other state of RuH or OsH, and neither is it caused by the omission of any further state in our calculations which might perhaps be nearly-degenerate with the $^4\Delta$ state. In preliminary single-reference CI(SD) calculations on OsH with our WB-MEFIT-PP we found no increase of the bond length for the $^4\Delta$ state, but rather a decrease of 0.18 a_0. Thus, although there is not yet any explanation for this unexpected and strange behaviour, it is certainly not due to a pseudopotential defect but rather to peculiarities of the correlation treatment. The quartet states of OsH show rather large dipole moments while the sextet states are comparably low polar states, due to the different molecular electronic configuration, and the hydrogen atom is the negatively polarized part of the molecular in all seven examined states.

The relativistic effects become visible when the data obtained with the HF-MEFIT-PP are compared with those obtained with the WB-MEFIT-PP. The bond distances are shortened for all seven states, although the relativistic contributions to the dissociation energies are not as uniform as they were in the case of RuH. Some states are lowered in their energy while others are raised depending on the level of the theoretical treatment. However, it must be kept in mind that the change in the Os ground state, which is also a relativistic effect, is also included in these data. Further effects of relativity are the increase of the vibrational frequencies and the changes of the polarity of the seven states, and these are similar to the changes found for the RuH states. Nevertheless, the results obtained with the two different RPPs show only rough agreement. A major difference between the two RPPs is manifested in the values for the dissociation energies D_e and is immediately visible from Fig. 2. In the CASSCF calculations with the WB-MEFIT-PP all quartet states are lower than the sextet states, with the $^4\Sigma^-$ state being the ground state. The correlation treatment then leads to a $^4\Pi$ ground state and to a lowered $^6\Sigma^+$ state which is nearly degenerate with the $^4\Delta$ state at the MRCI(SD) level and with the $^4\Phi$ state at the MR-CI(SD) + Q level. The HW-RECP, on the other hand, leads at the CASSCF level to quartet and sextet states which are not separated into two blocks and which lie within 4000 cm^{-1} of each other. The $^4\Pi$ state is already the ground state, while the $^4\Phi$ state becomes the highest state in this sequence, $^4\Delta$ and $^6\Sigma^+$ are nearly degenerate and lie slightly above the $^4\Sigma^-$ state. The $^4\Pi$ state remains the ground state at the MRCI(SD) level, followed now by the $^6\Sigma^+$ state, while the $^6\Pi$ state becomes the highest state and the $^4\Delta$ state is raised so high that it lies now between the $^4\Phi$ and $^6\Delta$ states. With inclusion of the size-consistency correction the $^4\Delta$ state becomes the highest state, while the remaining part of the term sequence is left unchanged.

These discrepancies in the description of the molecular electronic structure of OsH may result from the shortcomings of the HW-RECP in describing the

atomic electronic structure of Os [4], i.e., atomic excitation energies show errors of up to 0.88 eV. The differences in molecular excitation energies compared with the results obtained with the WB-MEFIT-PP are the same magnitude as in the case of the osmium atom [4]. We therefore suppose the $^4\Pi$ state to be the ground state of OsH, and conclude that there are at least two reasons why the WB-MEFIT-PP is superior to the HW-RECP for describing the molecular electronic structure of OsH: first because the WB-MEFIT-PP for Os is of the same quality as the WB-MEFIT-PP for Ru [4] and therefore may succeed in the simple molecular environment of the hydride as the Ru-pseudopotential did for RuH (see above), and second because the HW-RECP has severe difficulties in describing the atomic electronic structure and therefore may fail to describe the molecular electronic structure. In any case, the only way to answer unequivocally the question for the OsH ground state and its detailed molecular electronic structure would be either the application of further, differently adjusted and high quality pseudopotentials, or a thorough experimental examination of the OsH molecule.

4. Conclusion

Nonrelativistic and quasirelativistic energy-adjusted *ab initio* pseudopotentials for second and third row transition metal atoms [4] were tested on the ground states of the neutral and singly charged silver and gold dimers (Ag_2, Ag_2^+, Ag_2^- and Au_2, Au_2^+, Au_2^-) and on seven low-lying quartet and sextet states of ruthenium- and osmiummonohydride (RuH and OsH). These calculations used a shorter analytical expansion than earlier pseudopotentials for second row transition metal atoms [6], but had the same quality in atomic calculations, and with the corresponding optimized GTO valence basis sets. The spectroscopic constants R_e, D_e, and ω_e for the ground states of the silver and gold dimeric species and the ionization potentials and electron affinities for Ag, Au, Ag_2, and Au_2 were determined in CI(SD) and CEPA1 calculations, and the values obtained were in good agreement with the published theoretical values. In the case of the monohydrides, pseudopotentials published by other groups were also used for comparison in state-averaged CASSCF and MRCI(SD) calculations, and the spectroscopic constants, dipole moments and dipole derivatives were determined. For the seven electronic states $^4\Sigma^-$, $^4\Pi$, $^4\Delta$, $^4\Phi$, $^6\Sigma^+$, $^6\Pi$, and $^6\Delta$ of RuH, relativistic effects on the bond distances and the dissociation energies were determined and the same description of the molecular electronic structure was obtained with two different relativistically corrected pseudopotentials, indicating a certain convergence in the quantum chemical description of the molecule. All pseudopotentials employed for Ru led to a $^4\Sigma^-$ state as ground state of RuH. For OsH no other theoretical study is known. The same seven electronic states as in the case of RuH were investigated with a nonrelativistic and two relativistically corrected pseudopotentials; one of the latter were taken from the literature and did not perform well in atomic calculations. The results for OsH do not show the same agreement as in the case of RuH; the pseudopotential from literature, for example, gives a completely different term sequence, probably reflecting the same shortcomings as in atomic calculations. Despite these differences, we predict a $^4\Pi$ ground state for OsH since this is found with both of the relativistically corrected pseudopotentials, although a final answer requires further theoretical and, especially, experimental investigation of the OsH molecule.

Acknowledgements. We want to thank Prof. H.-J. Werner, Universität Bielefeld, for providing us with the program package MOLPRO and giving helpful advice for its implementation on the CRAY-2 in Stuttgart.

References

1. Krauss M, Stevens WJ (1984) Annu Rev Phys Chem 35:357
2. Wedig U, Dolg M, Stoll H, Preuss H (1986) Energy-adjusted pseudopotentials for transition-metal elements. In: Viellard A (ed) Quantum chemistry: the challenge of transition metals and coordination chemistry, NATO ASI Series C, vol 176. Reidel, Dordrecht, pp 79–89
3. Langhoff SR, Bauschlicher CW (1988) Annu Rev Phys Chem 39:181
4. Andrae D, Häußermann U, Dolg M, Stoll H, Preuss H (1990) Theor Chim Acta 77:123
5. Hay PJ, Wadt WR (1985) J Chem Phys 82:299
6. LaJohn LA, Christiansen PA, Ross RB, Atashroo T, Ermler WC (1987) J Chem Phys 87: 2812
7. Langhoff SR, Davidson ER (1974) Int J Quantum Chem 8:61
8. Martin RL (1987) J Chem Phys 86:5027
9. Moore CE (1958) Atomic energy levels, vol. 3. Nat Bur Stand (US) Circ. No. 467
10. Huzinaga S (1965) J Chem Phys 42:1293
11. Werner HJ, Universität Bielefeld, West Germany, Knowles PJ, University of Sussex, UK (1989) Program package MOLPRO, CRAY-2 version. See also Werner HJ, Knowles PJ (1985) J Chem Phys 82:5053; Knowles PJ, Werner HJ (1985) Chem Phys Lett 115:259 for details about the MCSCF program and Werner HJ, Knowles PJ (1988) J Chem Phys 89:5803: Werner HJ, Knowles PJ (1988) Chem Phys Lett 145:514 for details about the CI program
12. Hotop H, Lineberger WC (1985) J Phys Chem Ref Data 14:731
13. Basch H (1980) Faraday Symp R Soc Chem 14:149
14. Lee YS, Ermler WC, Pitzer KS (1980) J Chem Phys 73:360
15. Hay PJ, Martin RL (1985) J Chem Phys 83:5174
16. Ross RB, Ermler WC (1985) J Phys Chem 89:5202
17. Walch SP, Bauschlicher CW, Langhoff SR (1986) J Chem Phys 85:5900
18. Brown CM, Ginter ML (1978) J Mol Spectrosc 69:25
19. Bauschlicher CW, Langhoff SR, Partridge H (1989) J Chem Phys 91:2412
20. Chong DP, Langhoff SR (1986) J Chem Phys 84:5605
21. Balasubramanian K, Feng PY (1989) Chem Phys Lett 159:452
22. Ermler WC, Christiansen PA, private communication cited in [21]
23. Schwerdtfeger P, Dolg M, Schwarz WHE, Bowmaker GA, Boyd PDW (1989) J Chem Phys 91:1762
24. Ramirez-Solis A, Daudey JP, Novaro O, Ruiz ME (1990) Z. Phys. D 15:71
25. Huber KP, Herzberg G (1979) Constants of diatomic molecules. Van Nostrand–Reinhold, New York
26. Tolbert MA, Beauchamp JL (1986) J Phys Chem 90:5015
27. Krauss M, Stevens WJ (1985) J Am Chem Soc 107:4385
29. Langhoff SR, Pettersson LGM, Bauschlicher Jr CW, Partridge H (1987) J Chem Phys 86:268
30. Balasubramanian K, Wang JZ (1990) Chem Phys 140:243